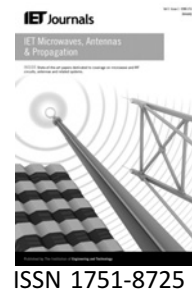


Published in IET Microwaves, Antennas & Propagation  
Received on 5th May 2009  
Revised on 27th December 2009  
doi: 10.1049/iet-map.2009.0278



# Behavioural modelling and impact analysis of physical impairments in quadrature modulators

M. Li<sup>1</sup> L. Hoover<sup>2</sup> K.G. Gard<sup>3</sup> M.B. Steer<sup>3</sup>

<sup>1</sup>FutureWei Technologies Inc., 1700 Alma Drive, Suite 500, Plano, TX 75075, USA

<sup>2</sup>Polyphase Microwave, Inc., 1111 W. 17th Street, #200, Bloomington, IN 47404, USA

<sup>3</sup>Department of Electrical and Computer Engineering, North Carolina State University, Campus Box 7914, Raleigh, NC 27695, USA

E-mail: minsheng.li@ieee.org

**Abstract:** Non-linear distortion and linear static errors (DC offset and gain/phase imbalance) are the major analogue impairments in microwave I/Q quadrature modulators. They can adversely impact the performance of the systems using them, especially for direct-conversion transceiver systems. The impacts of these impairments were investigated for three different modulator applications: double sideband modulation, zero intermediate frequency (IF) single sideband (SSB) orthogonal frequency-division multiplexing (OFDM) modulation and low-IF SSB OFDM modulation. A behavioural model for characterising the non-linear response and the linear static errors was developed. The non-linear characteristic of each input was modelled by a complex power series based on amplitude-to-amplitude modulation and amplitude-to-phase modulation measurements. The linear static errors were modelled as three static error terms added into the complex power series based on a four-DC-point vector network analyser measurement. The non-linear model was validated by measurements with three types of signals representing the three modulator applications.

## 1 Introduction

Owing to high spectral efficiency, analogue quadrature modulators and demodulators are widely used in radio frequency (RF) transceivers to save cost, especially for wideband applications. Analogue imperfections in modulators and demodulators include the non-linearity, DC offset, quadrature gain/phase imbalance, phase noise, frequency error, and so on. They can degrade the system performance by producing spurious or noise components. The DC offset and gain/phase imbalance are especially serious problems in a direct-conversion transceiver system.

The two main system specifications impacted by static modulator errors and non-linear distortion are spectral emissions mask, which defines the allowable signal levels outside of the signal bandwidth and signal waveform quality, which is represented as signal-to-noise and distortion ratio (SNDR), error vector magnitude (EVM) or

the correlation coefficient ( $\rho$ ). Modulator non-linearity generates intermodulation products in the form of spectral regrowth of the desired signal, which are new frequency components created by the creation of mixing products between the individual frequency components of the signal spectrum. Some of the new frequency components called out-of-band distortion fall outside the signal bandwidth and extend into the adjacent frequency bands causing degradation of the spectral mask performance; while others called in-band distortion are within the signal bandwidth contributing to SNDR degradation [1].

The linear static errors, DC offset and gain/phase imbalance, result from the device mismatches (device sizes, threshold voltage, etc.). The DC offset causes degradation by carrier feedthrough. The gain/phase imbalance generates unwanted image spectrum interfering with the desired signals. The impact of static modulator errors depends largely on how the modulator is used. For instance, for wideband code-division

multiple access (WCDMA) and zero intermediate frequency (IF) orthogonal frequency-division multiplexing (OFDM) systems, the static errors contribute only to SNDR degradation, although each of these systems is impacted differently. Interestingly, SNDR of low-IF OFDM systems are not impacted by static errors, but out-of-band emissions are impacted. Estimation and compensation for errors from DC offset and gain/phase imbalances were proposed in [2, 3].

Owing to the adverse impacts, it is important to develop a systematic approach fast and accurately to assess the analogue impairments in quadrature modulators for system evaluation and verification. As a compact representation of a circuit or a system, a behavioural model typically simulates much faster and requires less memory than its circuit-level counterpart, which makes it a powerful tool for system design and verification. Various behavioural models based on bandpass non-linearity concept and amplitude-to-amplitude (AM-AM) and amplitude-to-phase (AM-PM) extraction techniques have been developed by researchers for predicting the adjacent channel power ratio (ACPR) of power amplifiers [4–8]. Similar modelling approach was developed for quadrature modulators in [9] in characterising the non-linear distortion with an offset single-tone sinusoid AM-AM and AM-PM measurements.

In this paper, the impacts of analogue impairments in quadrature modulators on spectral regrowth and waveform quality were investigated for three different modulator applications: double sideband (DSB) modulation, zero-IF single sideband (SSB) OFDM modulation and low-IF SSB OFDM modulation. For the first time, a behavioural model based on [9] was developed to accurately characterise both non-linear distortion and linear static errors, including DC offset and gain/phase imbalance.

The paper is organised as follows. In Section 2, three application scenarios of quadrature modulators were reviewed and the different impacts of non-linear distortion, DC offset and gain/phase imbalance on these three modulator applications were investigated. In Section 3, the development of non-linear behavioural model for characterising both non-linear characteristics and linear static errors (DC offset and gain/phase imbalance) in quadrature modulators was described. In Section 4, the ACPR measurement results were presented to validate the non-linear behavioural model in predicting the out-of-band distortion. Finally, the findings were concluded in Section 4.

## 2 Impact analysis of physical impairments in three applications of quadrature modulators

Different wireless applications use different modulation schemes which utilise quadrature modulators in different ways. The applications of quadrature modulators can be found in three scenarios of wireless communications systems as discussed in the following sections.

### 2.1 DSB modulation systems

In many linear digital wireless systems such as DECT, EDGE, CDMA and WCDMA, variations of quadrature phase shift keying (QPSK) modulation are utilised where independent filtered data streams are inputs to the modulator. The independent inputs  $I$  and  $Q$  are up-converted to the carrier frequency by the  $I$  and  $Q$  channels, respectively. Each signal is directly converted up to RF as DSB modulation about the carrier; thus, the RF bandwidth is twice the baseband signal bandwidth. The two overlapping  $I$  and  $Q$  DSB signals are in quadrature which can be separated at the receiver using a quadrature demodulator; however, static errors cause the  $I$ -channel information to bleed into  $Q$ -channel, and vice versa, resulting in SNDR degradation which is proportional to the error.

### 2.2 Zero-IF SSB modulation systems

One property of quadrature modulator is that SSB modulation can be achieved if the  $I$  and  $Q$  inputs are the Hilbert transform of each other. For example, the quadrature modulators in OFDM modulation-based wireless communication systems such as wireless local area networks (WLAN) and worldwide interoperability for microwave access (WiMax) perform SSB modulation on each modulated sub-carrier of the OFDM signals.

There are two architectures for the OFDM systems. One is called zero-IF architecture, where the modulator is used to create independent sub-carriers in the upper and lower sidebands symmetrically about the RF carrier frequency. In this case, the baseband input data streams are a combination of data streams for both sidebands. The  $I$  and  $Q$  inputs of a zero-IF OFDM signal to quadrature modulators are generated by inverse fast Fourier transform (IFFT) to sum all the sub-carriers and the subsequent digital to analogue converters (DACs).

$$i(t) = \Re \left( \sum_{k=0}^{N-1} C_k(t) e^{j\omega_k t} \right) = \sum_{k=0}^{N-1} [I_k \cos(\omega_k t) - Q_k \sin(\omega_k t)]$$

$$q(t) = \Im \left( \sum_{k=0}^{N-1} C_k(t) e^{j\omega_k t} \right) = \sum_{k=0}^{N-1} [I_k \sin(\omega_k t) + Q_k \cos(\omega_k t)] \quad (1)$$

where  $C_k(t) = I_k(t) + jQ_k(t)$  represents the location of the symbols within the constellation for the  $k$ th sub-carrier at different symbol time. As expected,  $i(t)$  and  $q(t)$  of a zero-IF OFDM signal are Hilbert transform related.

### 2.3 Low-IF SSB modulation systems

The third case referred to as low-IF SSB modulation system is to use the modulator at a low-IF where the SSB modulation is up-converted to one sideband, either upper or lower, of the RF carrier. Low-IF OFDM transmitters have been researched in [10, 11], because it is less sensitive to the modulator's DC offset and gain/phase imbalance

compared to its zero-IF counterpart [12]. However, it requires at least double sampling rate for the DACs and suffers from increased adjacent channel interferences as discussed in the following sections.

Unlike zero-IF OFDM, a digital up-conversion takes place before the IFFT summation in low-IF OFDM architecture, which moves the baseband centre frequency from DC to  $\omega_{IF}$ . The inputs  $I$  and  $Q$  of a low-IF OFDM signal to quadrature modulators are described in (2).

$$i(t) = \Re \left( \sum_{k=0}^{N-1} C_k(t) e^{j\omega_k t} e^{j\omega_{IF} t} \right) \quad (2)$$

$$q(t) = \Im \left( \sum_{k=0}^{N-1} C_k(t) e^{j\omega_k t} e^{j\omega_{IF} t} \right)$$

For the three quadrature modulator applications, the impacts of DC offset, gain/phase imbalance and intermodulation distortion on the adjacent channel interference and signal quality are different as is illustrated in Fig. 1 and discussed in the following sections.

**2.3.1 Non-linear distortion:** Modulator non-linearity generates spectral regrowth both in-band and out-of-band, which can degrade the signal quality and interfere with the adjacent channels. Multi-tone signals are effective in estimating the in-band and out-of-band distortion in real communication signals [13, 14]. In this section, a four-tone (equal amplitude and zero-phase) analysis was conducted to investigate the impact of non-linear distortion in three quadrature modulator applications. Note that the use of equal amplitude and zero-phase multi-tone signal may over- or under-estimate the in-band or out-of-band distortion [13]; however, it suffices in this paper for the purpose of qualitatively analysing the impact of non-linear distortion in different modulator applications.

**Zero-IF OFDM systems:** To simulate the OFDM signal in the four-tone analysis, an in-phase and a quadrature four-tone sinusoidal signal were applied to  $I$  and  $Q$  channels, respectively, to produce a four-tone SSB RF output.

$$\begin{aligned} i(t) &= \cos(\omega_1 t) + \cos(\omega_2 t) + \cos(\omega_3 t) + \cos(\omega_4 t) \\ q(t) &= \sin(\omega_1 t) + \sin(\omega_2 t) + \sin(\omega_3 t) + \sin(\omega_4 t) \end{aligned} \quad (3)$$

where  $\omega_1, \omega_2, \omega_3$  and  $\omega_4$  are four equally spaced tones centred about  $\omega_{bc}$

$$\begin{aligned} \omega_1 &= \omega_{bc} - 3\Delta/2; & \omega_2 &= \omega_{bc} - \Delta/2 \\ \omega_3 &= \omega_{bc} + \Delta/2; & \omega_4 &= \omega_{bc} + 3\Delta/2 \end{aligned} \quad (4)$$

As described in Section 2.2, for zero-IF OFDM  $\omega_{bc} = 0$ .

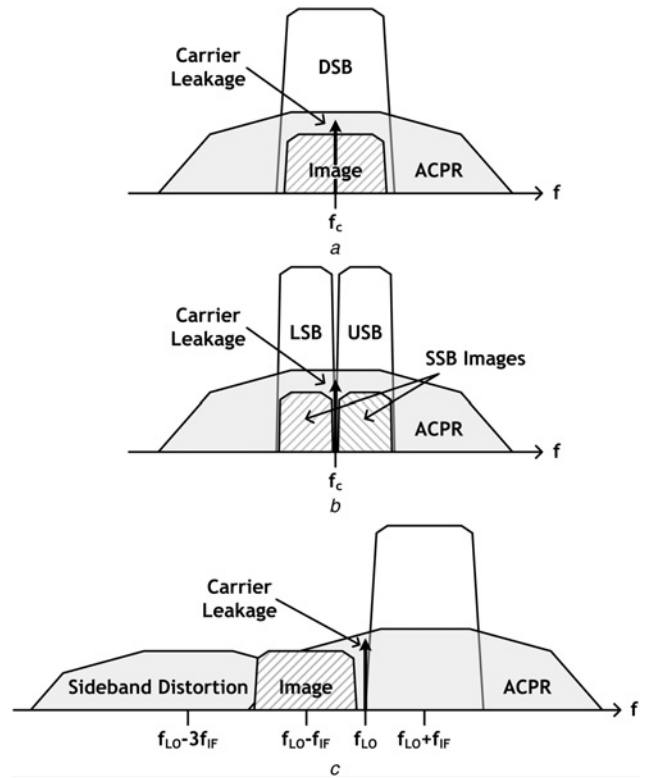


**Figure 1** Impact of static errors and non-linear distortion on different quadrature modulator applications

- a DSB quadrature
- b Zero-IF SSB (both upper sideband (USB) and lower sideband (LSB))
- c Low-IF SSB

Without loss of generality, a third-order non-linearity was assumed for  $I$  and  $Q$  channels.

$$G_I(x) = G_Q(x) = a_1 x + a_3 x^3, \quad x = i(t) \text{ or } q(t) \quad (5)$$

The modulator output  $v_{out}(t)$  becomes

$$v_{out}(t) = G_I(x) \cos(\omega_c t) + G_Q(x) \sin(\omega_c t) \quad (6)$$

By trigonometry, the modulator output including the desired signal components and all distortion components was computed and plotted in Fig. 2 for zero-IF OFDM systems.

**DSB modulation systems:** For DSB modulated signals, the baseband  $I$  and  $Q$  data are independent and the spectrum of  $I$  and  $Q$  data are overlapped on top of each other orthogonally. Therefore it is a valid simplification to examine the modulator output spectrum with only one channel on.

$$\begin{aligned} i(t) &= \cos(\omega_1 t) + \cos(\omega_2 t) + \cos(\omega_3 t) + \cos(\omega_4 t) \\ q(t) &= 0 \end{aligned} \quad (7)$$

The four-tone analysis for DSB modulated signals shows very similar spectrum results around the carrier frequency as the zero-IF OFDM signals. However there is a subtle distinction

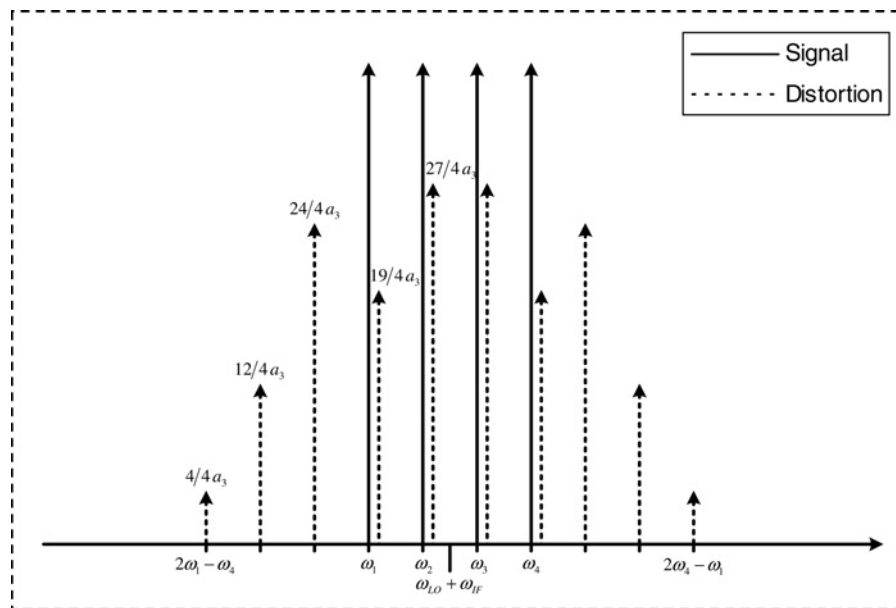


**Figure 2** Four-tone analysis for zero-IF OFDM: calculated modulator output spectrum terms

that for zero-IF OFDM systems, the desired signal and the corresponding distortion terms are SSB while both are DSB for DSB modulation case. The important observation is that for DSB modulation case the ratio between the signal and the distortion terms remains the same as that for the zero-IF OFDM case. Therefore it can be concluded that if a zero-IF OFDM signal such as a WLAN signal and a DSB modulated signal such as a CDMA or WCDMA signal have similar peak-to-average ratio (PAR), they should produce similar amount of in-band distortion if no significant memory exists in the quadrature modulator. It is worth mentioning that signals with the same PAR will not necessarily generate the same level of in-band distortion (dBc) because two signals with the same PAR may also have differences in amplitude distribution between the average and peak values. However, it has been shown that both CDMA and WCDMA base-station signals, including many

orthogonal code channels and WLAN OFDM signals, have statistical properties that are similar to complex Gaussian signals [15, 16] and therefore these signals generate similar levels of out-of-band and in-band distortion if they have similar PAR.

*Low-IF OFDM systems:* The four-tone SSB signal model as described in (3) and (4) was used to model the low-IF OFDM signal by setting  $\omega_{bc} = \omega_{IF}$ . Assuming a third-order non-linearity as described in (5), the modulator output, including the desired signal components and all distortion components, was calculated and plotted in Fig. 3 for low-IF OFDM systems.

An interesting observation from the analysis results as illustrated in Figs. 2 and 3 is that in the low-IF OFDM case, a portion of the third-order intermodulation

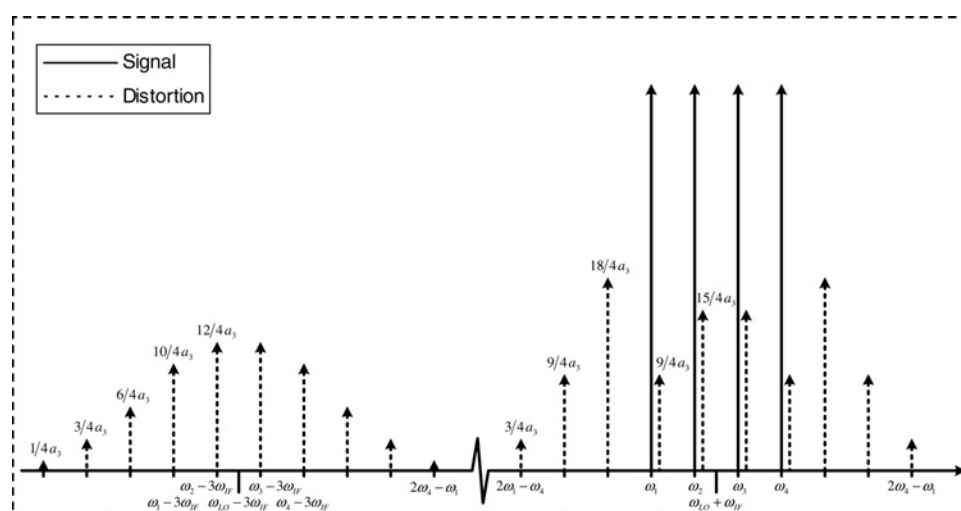


**Figure 3** Four-tone analysis for low-IF OFDM: calculated modulator output spectrum terms

distortion power is shifted to the third IF harmonic sideband centred at  $\omega_{LO} - 3\omega_{IF}$ . The total distortion power is the same as the zero-IF case, but the distortion about the desired sideband is reduced 2.5 dB for the four-tone uniform phase test signal. Example modulator output spectrums for zero-IF and low-IF OFDM are shown in Fig. 4. This leads to the following conclusions:

1. In low-IF OFDM, modulator non-linearity results in less in-band distortion because of the distortion split, which means better SNDR/EVM than its zero-IF counterpart. The drawback is the increased interferences to the channels around the third-IF harmonic at  $\omega_{LO} - 3\omega_{IF}$ .
2. Unlike zero-IF OFDM, the modulator output spectrum of low-IF OFDM signals is not symmetrical around the RF carrier – there is a spectrum hump in the third lower sideband, which leads to asymmetrical ACPR.

The above analysis results were verified by EVM measurements using three types of wireless signals: (i) WCDMA uplink pilot signal and WCDMA downlink test model 5 signal (a standard WCDMA base-station conformance testing signal [17]), which represent the DSB modulation systems; (ii) zero-IF WLAN signal with 16 QAM OFDM modulation which represents the zero-IF SSB modulation systems and (iii) low-IF WLAN signal with 16 QAM OFDM modulation which represents the low-IF SSB modulation systems. The downlink WCDMA

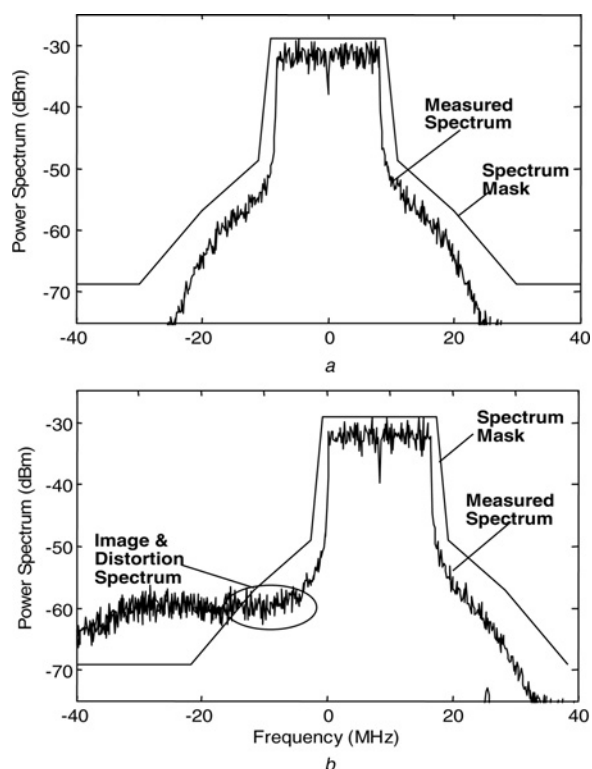


**Figure 4** Measured output spectrum

- a Zero-IF WLAN signal  
b Low-IF WLAN signal

test model 5 signal and the zero-IF and low-IF WLAN signals have a similar PAR of approximately 11 dB, while the WCDMA uplink pilot signal has a smaller PAR of 3.4 dB. As shown in Fig. 5, the EVM excited with the WCDMA downlink signal and the zero-IF WLAN signal are very close (the large discrepancy in the linear region is due to the higher noise floor in the generated WCDMA signals), while they are worse than the low-IF OFDM case. In addition, the WCDMA uplink signal has a much better EVM than other signals due to its smaller PAR. The measurement results validate the above analysis.

**2.3.2 DC offset:** Carrier feedthrough caused by device mismatches in quadrature modulators and direct leakage paths is a major concern in designing direct-conversion transceivers. A DC offset leads to a modulation constellation offset in DSB modulation systems [18]. In the up-converter, the mismatch can be modelled as a DC offset in the baseband input signals, which is up-converted to the carrier frequency. The resulting carrier leakage (CL) is an interference uncorrelated to the input signals if the carrier falls within the bandwidth of the receive signal. Therefore together with the noise, the CL term will degrade the SNDR of the system. The degradation of the SNDR due to the DC offset can be estimated using (8).

$$\text{SNDR} = 10 \log \left( \frac{\text{signal power}}{\text{carrier leakage} + \text{noise}} \right) \quad (8)$$

To validate the relationship of SNDR and CL in (8) experimentally, a sweeping DC offset was intentionally introduced in the quadrature modulator excited by an uplink WCDMA signal and the modulator output EVM was measured because SNDR and EVM are mathematically related [19]. As shown in Fig. 6, the measured and calculated EVM based on (8) are close within 1%, indicating

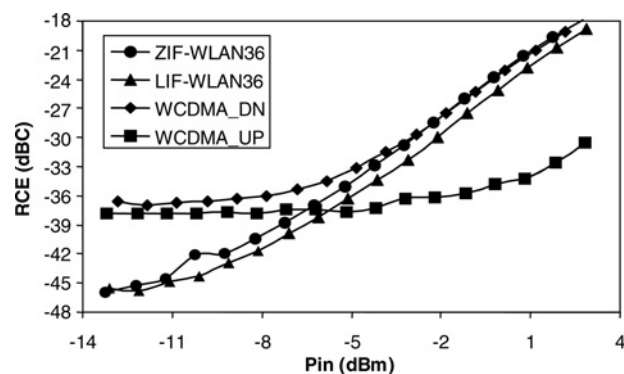


**Figure 5** Measured EVM against input power ( $P_{in}$ ) using three types of signals: (1) WCDMA uplink pilot signal (WCDMA\_UP) and WCDMA downlink test model 5 signal (WCDMA\_DN); (2) zero-IF WLAN signal with 16 QAM OFDM modulation (ZIF\_WLAN36) and (3) low-IF WLAN signal with 16 QAM OFDM modulation (LIF\_WLAN36)

An equivalent term as EVM, relative constellation error (RCE) was used here.  $\text{RCE} = 20 \log(\text{EVM})$

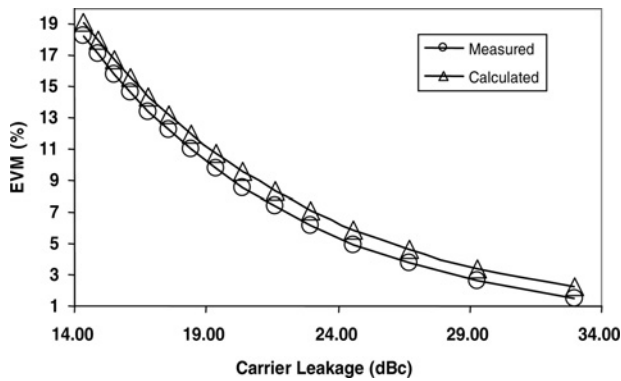


**Figure 6** Measured and calculated EVM against CL using a WCDMA uplink signal

that (8) can be used to accurately estimate the SNDR degradation due to the CL.

In a WLAN or WiMax system utilising zero-IF OFDM modulation, usually the OFDM sub-carrier at RF carrier frequency is not used in order to eliminate the adverse impact of the DC offset as mentioned before. However, the DC offset can still cause interferences to adjacent sub-carriers at the receiver due to the frequency offset [20], which degrades the received signal quality.

The second advantage of a low-IF OFDM architecture is its immunity to the DC offset at both transmitter and receiver sides because all the modulated sub-carriers are moved away from the RF carrier, as shown in Fig. 1c. Therefore CL presented at the input of the receiver will not cause interference to the received signal. However, the CL becomes out-of-band emission which will degrade the spectral emission mask performance.

**2.3.3 Gain/phase imbalance:** Quadrature gain/phase imbalance produces image spectrum uncorrelated to the signals that will either degrade the signal SNDR or increase the adjacent channel interference depending on the applications of the quadrature modulators.

*DSB modulation systems:* In a DSB modulation system, the gain/phase imbalance distorts the signal constellation: the gain imbalance changes the constellation from square to rectangular, whereas the phase imbalance causes skew of the constellation [18]. Skew of the constellation can be viewed as part of the  $I$ -channel being projected on the  $Q$ -channel, and vice versa. In the frequency domain, the gain/phase imbalance produces image spectrum within the signal bandwidth, which is uncorrelated to the signals because the  $I$  and  $Q$  data streams are independent. Therefore the image spectrum impacts the signal quality by degrading the system SNDR. If the thermal noise of the modulator is negligible compared to the image power, we expect

$$\text{SNDR} = 10 \log \left( \frac{\text{signal power}}{\text{image power} + \text{noise}} \right) \approx \text{IRR} \quad (9)$$

where IRR is the image rejection ratio (IRR) [21].

$$\text{IRR} = 10 \log \left( \frac{1 + 2\sqrt{\Delta} \cos(\theta) + \Delta}{1 - 2\sqrt{\Delta} \cos(\theta) + \Delta} \right) \quad (10)$$

where  $\theta$  is the phase difference in degree between  $I$  and  $Q$  and  $\Delta$  is the ratio square of the amplitude of  $I$  to  $Q$  channels.

*Zero-IF OFDM systems:* Instead of distorting the signal constellations in a DSB modulation system, the gain/phase imbalance causes the state spreading of the zero-IF OFDM signal constellations (like what phase noise does) because of the total effects of multiple sub-carriers [18]. Equations (9) and (10) can also be used to predict the SNDR degradation due to gain/phase imbalance for zero-IF OFDM signals because they can be viewed as multiple SSB modulated sub-carriers distributed symmetrically around the RF carrier.

The relationship between IRR and SNDR as described in (9) and (10) for DSB modulation systems and zero-IF OFDM systems was validated by a MATLAB simulation. In the simulation, the quadrature modulator behavioural model developed in Section 3 was used to calculate the modulator output with real WCDMA and zero-IF WLAN signals. A sweeping gain/phase imbalance was deliberately introduced into the modulator model, while the CL and non-linear distortion were kept at a negligible level. Cross-correlation between the model input and output was calculated to determine the uncorrelated spectrum so that the SNDR can be calculated. As shown in Fig. 7, the calculated IRR and the simulated SNDR for WCDMA and zero-IF WLAN signals are very close within 0.1 dB for a combined range of gain errors (0.1–2 dB) and phase errors (1–20°), which validates (9) and (10) for DSB modulation systems and zero-IF OFDM systems.

However, for zero-IF OFDM signals, 3 dB worse SNDR than that predicted by (9) and (10) was observed in laboratory measurements. The apparent reason appears to be the complexity of the baseband equaliser utilised for the WLAN standard. A more complicated channel equalisation filter recovers the 3 dB difference for the zero-IF OFDM signals. It is important to note that WLAN transceivers are designed for the 3 dB tougher case; thus, given same SNDR degradation, the amplitude and phase balance requirements for zero-IF OFDM systems are more stringent than DSB modulation systems.

Equations (9) and (10) were further validated by lab measurements. A sweeping gain/phase imbalance was deliberately introduced to the modulator and the EVM of the modulator output was measured when using a WCDMA downlink signal and a 64-QAM zero-IF WLAN signal. The calculated IRR contour over gain/phase imbalance and the measured EVM were compared in

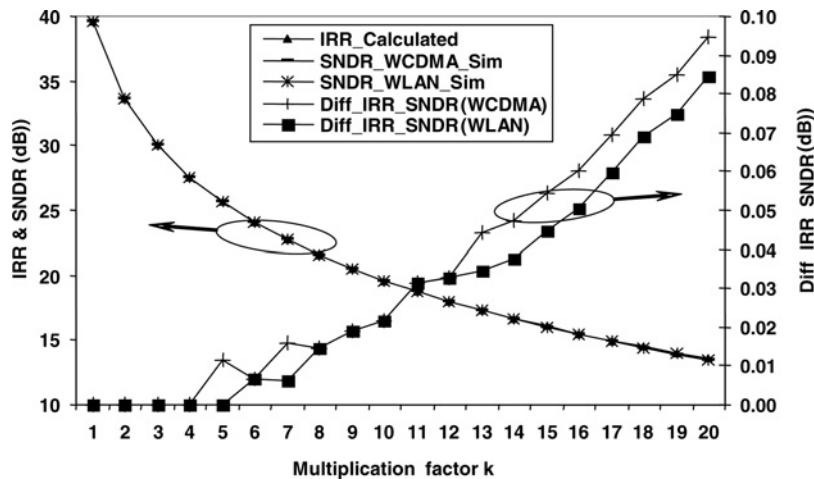


**Figure 7** Calculated IRR (*IRR\_Calculated*) against simulated SNDR for WCDMA (*SNDR\_WCDMA\_Sim*) and zero-IF OFDM (*SNDR\_WLAN\_Sim*) signals with gain and phase errors (gain error = 0.1 k dB, phase error = 1 k degree)

Left axis: absolute value of calculated IRR and simulated SNDR; Right axis: difference between calculated IRR and simulated SNDR for WCDMA (*Diff\_IRR\_SNDR (WCDMA)*) and WLAN (*Diff\_IRR\_SNDR (WLAN)*)

**Fig. 8.** Given the same gain/phase imbalance, the measured EVM of zero-IF WLAN signal is 3 dB worse than that of WCDMA signal because of the above-mentioned reason. The measured EVM for both signals has a good match with the calculated IRR (zero-IF WLAN with 3 dB offset), which consolidate the method to use (9) and (10) to predict the waveform quality degradation due to the gain/phase imbalance for both DSB modulated signals and zero-IF SSB modulated signals.

*Low-IF OFDM systems:* Unlike DSB modulated and zero-IF OFDM signals, low-IF OFDM signals are much less sensitive to gain/phase imbalance because all the SSB modulated sub-carriers are up-converted to one sideband,

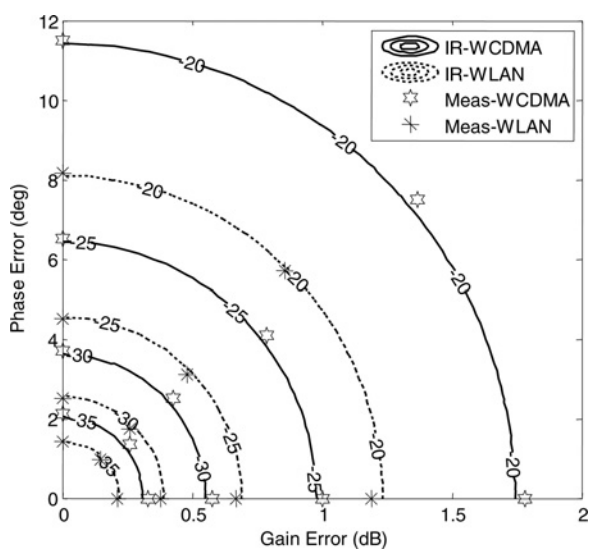


**Figure 8** Measured EVM contours for WCDMA (*Meas-WCDMA*) and zero-IF WLAN (*Meas-WLAN*) and calculated IR contours for WCDMA (*IR-WCDMA*) and zero-IF WLAN (*IR-WLAN*) against gain/phase error

as discussed in Section 2.3. Therefore the image spectrum is in the opposite sideband instead of the signal band. As shown in **Fig. 9**, trace (1) shows the measured spectrum of a real low-IF WLAN signal ( $f_{LO} = 3.4$  GHz) without quadrature imbalance, with all the sub-carriers in the upper sideband. Trace (2) shows the measured spectrum for the same signal with certain gain/phase imbalance introduced. It is obvious that the image spectrum is out of the signal band and thus would not cause SNDR/EVM degradation, which is the third advantage of low-IF OFDM architecture besides less in-band distortion and the immunity to DC offset as discussed in Sections 2.2.1 and 2.2.2.

However, low-IF OFDM architecture has two drawbacks. First, the image spectrum is out-of-band and part of the in-band distortion is shifted out-of-band, which introduces more adjacent channel interferences. This means more efforts are needed to meet the spectrum mask specification. An interesting observation is that if considering only gain/

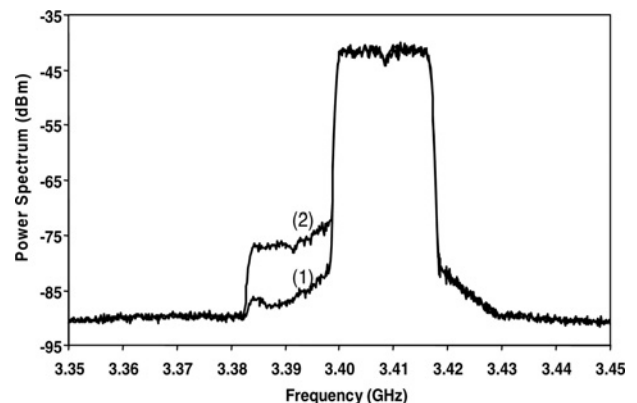


**Figure 9** Measured spectrum of a low-IF WLAN signal: (1) without gain/phase imbalance; (2) with gain/phase imbalance

phase imbalance, in low-IF WLAN systems, because the image spectrum is out-of-band, with as small as 0.2 dB gain error or 2° phase error, the spectrum mask will be violated. However, as shown in Fig. 8, in zero-IF WLAN systems it requires at least 0.7 dB gain error or 4.6° phase error to exceed the worst-case EVM (−25 dB for WLAN). This means more stringent gain/phase imbalance specification is required for low-IF OFDM systems in order to meet the spectrum mask than that for zero-IF OFDM systems to meet the EVM requirement. Second, the implementation cost is higher than the zero-IF OFDM systems because the sampling rate of the DACs in the low-IF OFDM systems has to be at least doubled.

### 3 Linear and non-linear behavioural model

Behavioural modelling is an efficient approach to characterise the non-linear distortion of non-linear devices. To the author’s best knowledge, litter research work has been done for behavioural modelling of quadrature modulators. In this section, a behavioural model was developed for characterising both non-linear distortion and linear static errors (DC offset and gain/phase imbalance) for a passive microwave quadrature modulator manufactured by PolyPhase Microwave Inc. It is worth mentioning that the modelling methodology is applied to generic quadrature modulators.

#### 3.1 Model structure

Quadrature modulators typically implement separate amplifiers and mixers for the in-phase and quadrature signal paths prior to the RF combiner; thus the two paths are considered isolated from each other either electronically, for example, double balanced Gilbert cell mixers or electrically through hybrid couplers. Therefore the non-linear characteristic of  $I$  and  $Q$  channels of the modulator can be modelled as a sum of two bandpass non-linearities that are described as the sum of two complex power series. This leads to the baseband equivalent model of the quadrature modulator as shown in Fig. 10, where  $\tilde{G}_I$  and  $\tilde{G}_Q$  are complex transfer characteristics of the up-converting circuitry of  $I$  and  $Q$  channels, respectively, both described as envelope complex power series [9]. The model result is the envelope of the modulator RF output, which can be obtained by the quadrature summation of the

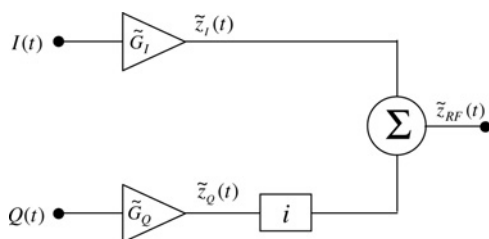


Figure 10 Baseband equivalent non-linear model of quadrature modulator

envelopes of the  $I$  and  $Q$ -channel outputs

$$\tilde{z}_{RF}(t) = \tilde{z}_I(t) + j\tilde{z}_Q(t) \tag{11}$$

The non-linear behavioural model [9] was extended in this paper to be able to accurately capture both non-linear distortion and linear static errors. The DC offset and gain/phase imbalance are modelled as three add-on coefficients  $a_{I,0}/a_{Q,0}$ ,  $\delta$  and  $\theta$  that are added into the two complex power series, as shown in (12) and (13).

$$\tilde{z}_I(t) = \tilde{G}_I[I(t)] = a_{I,0} + \tilde{a}_{I,1}I + \sum_{n=3, \text{odd}}^N \tilde{a}_{I,n}I^n \tag{12}$$

$$\tilde{z}_Q(t) = \tilde{G}_Q[Q(t)] = a_{Q,0} + \tilde{a}_{Q,1}\delta e^{j\theta}Q + \sum_{n=3, \text{odd}}^N \tilde{a}_{Q,n}Q^n \tag{13}$$

where  $\tilde{a}_{I,n}$  and  $\tilde{a}_{Q,n}$  are the complex power-series coefficients characterising the non-linear response of the  $I$  and  $Q$  channels. These coefficients were extracted by an offset single-tone sinusoid AM–AM and AM–PM measurement and least-square curve fitting [9]. The coefficients  $a_{I,0}/a_{Q,0}$ ,  $\delta$  and  $\theta$  characterise the DC offset, amplitude imbalance and phase imbalance between the  $I$  and  $Q$  channels, respectively. These three static error coefficients are extracted using a four-point vector network analyser (VNA) measurement as described in the next section.

#### 3.2 Linear static errors modelling

A four-point VNA measurement was conducted to extract the three model coefficients characterising the DC offset and gain/phase imbalance. Four DC inputs to the quadrature modulator are

- (1)  $I = +B, Q = 0$ ; (2)  $I = 0, Q = +B$
- (3)  $I = -B, Q = 0$ ; (4)  $I = 0, Q = -B$

The input voltage setting,  $B$ , was chosen as 100 mV in order to operate the modulator well within the linear region and thus the non-linear phenomenon is negligible. Under this condition, the modulator envelope output is

$$\tilde{G}_I[I(t)] = a_{I,0} + \tilde{a}_{I,1}I = a_{I,0} + (x_{I,1} + jy_{I,1})I \tag{14}$$

$$\tilde{G}_Q[Q(t)] = a_{Q,0} + \tilde{a}_{Q,1} \cdot \delta \cdot e^{j\theta}Q = a_{Q,0} + (x_{Q,1} + jy_{Q,1})Q \tag{15}$$

Combining (11), (14) and (15) we obtain

$$\tilde{z}_{RF}(t) = (a_{I,0} + x_{I,1}I - y_{Q,1}Q) + j(a_{Q,0} + y_{I,1}I + x_{Q,1}Q) \tag{16}$$

The output complex envelopes were measured using a VNA. Denote the real and imaginary parts of the output complex envelopes as  $\tilde{I}_0, \tilde{I}_1, \tilde{I}_2, \tilde{I}_3$  and  $\tilde{Q}_0, \tilde{Q}_1, \tilde{Q}_2, \tilde{Q}_3$ . By

equating the real and imaginary parts in (16) for the four measurement points, we have

$$a_{I,0} = \frac{1}{4} \sum_{i=0}^3 \tilde{I}_i \quad a_{Q,0} = \frac{1}{4} \sum_{i=0}^3 \tilde{Q}_i \quad (17)$$

$$x_{I,1} = (\tilde{I}_0 - \tilde{I}_2)/(2B) \quad y_{I,1} = (\tilde{Q}_0 - \tilde{Q}_2)/(2B)$$

$$x_{Q,1} = (\tilde{Q}_1 - \tilde{Q}_3)/(2B) \quad y_{Q,1} = -(\tilde{I}_1 - \tilde{I}_3)/(2B)$$

Knowing  $a_{I,0}$ ,  $a_{Q,0}$ ,  $x_{I,1}$ ,  $y_{I,1}$ ,  $x_{Q,1}$ ,  $y_{Q,1}$ , the gain/phase error terms ( $\delta$  and  $\theta$ ) and CL can be calculated as

$$\delta = \frac{|x_{Q,1} + jy_{Q,1}|}{|x_{I,1} + jy_{I,1}|}$$

$$\theta = \angle(x_{Q,1} + jy_{Q,1}) - \angle(x_{I,1} + jy_{I,1}) \quad (18)$$

$$CL(\text{dBm}) = 10 \log\left(\frac{a_{I,0}^2 + a_{Q,0}^2}{50}\right) + 30$$

The four-point measurement is able to extract all the linear errors model coefficients utilising only a DC voltage source and a VNA with four easy measurements. This extraction approach was validated by the SSB image rejection (IR) and CL measurements. A SSB sinusoidal signal was applied to the modulator inputs at a RF of 3.4 GHz. The IR and CL were measured and compared with the modelled results. They are in good agreement with a discrepancy less than 1 dBc, which indicates that the four-point measurement is an accurate approach to extract the model coefficients for the modulator static errors.

The complete model parameters for the quadrature modulator at 3.4 GHz are presented in Table 1. The complex power series coefficients  $\tilde{b}_{I,i}$  and  $\tilde{b}_{Q,i}$  of order  $N=11$  characterise the  $I$  and  $Q$ -channel non-linear responses; the real coefficients  $a_{I,0}/a_{Q,0}$  characterises the DC offset;  $\delta$  and  $\theta$  characterise the gain/phase errors.

## 4 Simulation and measurement results

The non-linear behavioural model of quadrature modulators was validated through measurements using three wireless signals, WCDMA, zero-IF WLAN and low-IF WLAN, which represents the three applications discussed in Section 2: DSB modulation, zero-IF SSB OFDM modulation and low-IF SSB OFDM modulation systems. The out-of-band distortion of the modulator was characterised by the ACPR measurement. ACPR is a key figure-of-merit in quantifying the adverse impact of spectral regrowth on the adjacent channels. Different communication signals have different ACPR specifications. In WCDMA systems, a slightly different name, adjacent channel leakage ratio (ACLR) is used and defined as the ratio of the total power within the desired information bandwidth to the total power in an adjacent channel bandwidth, with a frequency

**Table 1** Non-linear behavioural model coefficients

Static linear errors	DC offset	$a_{I,0}$	0.0017
		$a_{Q,0}$	0.0014
	Gain err	$\delta$	1.0045
	Phi Err, (deg)	$\theta$	-0.3313
nonlinear responses		$b_{I,1}$	-0.05842 + 0.47786i
		$b_{I,3}$	0.21239 + 0.046232i
		$b_{I,5}$	-0.20392 - 1.0439i
		$b_{I,7}$	0.004129 + 1.5826i
		$b_{I,9}$	0.090961 - 1.0033i
		$b_{I,11}$	-0.035703 + 0.23708i
		$b_{Q,1}$	-0.05842 + 0.47786i
		$b_{Q,3}$	0.13421 + 0.038073i
		$b_{Q,5}$	0.16119 - 0.9349i
		$b_{Q,7}$	-0.6273 + 1.3725i
		$b_{Q,9}$	0.57698 - 0.84178i
		$b_{Q,11}$	-0.17532 + 0.19214i

offset away from the carrier frequency by (i) 5 MHz and (ii) 10 MHz [22].

In this section, two WCDMA signals were applied to the quadrature modulator and its non-linear behavioural model: (i) an uplink pilot signal; (ii) a downlink test model 5 signal. The modelled and measured ACLR at 5 MHz offset were compared. Fig. 11 shows the measured against the modelled lower sideband ACLR. There is an excellent agreement (within 1 dB difference) between the measured and modelled ACLR, indicating that the non-linear model predicts the out-of-band distortion of the quadrature

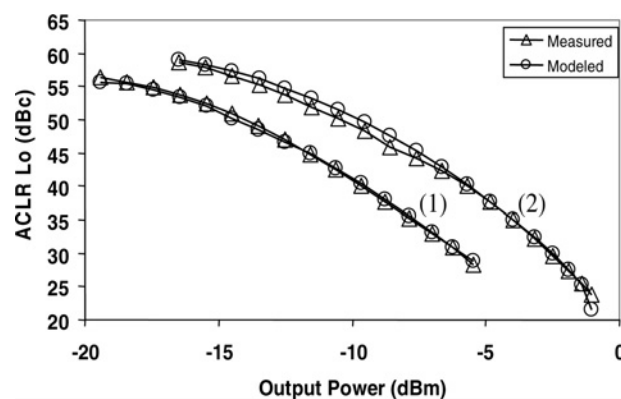


**Figure 11** Measured and modelled ACLR (lower sideband): (1) WCDMA downlink test model 5 signal; (2) WCDMA uplink pilot signal

modulator in the DSB modulation applications very accurately. The ACLR of the upper and lower sideband are very close for both measured and modelled results. This symmetry indicates that there is no significant memory in the modulator.

For WLAN signals, there is no explicit ACPR definition [23] because EVM is the more stringent metric. For the purpose of model validation in characterising out-of-band distortion, in this paper, an ACPR is defined for WLAN signals as the ratio of the total power within the desired 20 MHz bandwidth to the total power in an adjacent 20 MHz channel bandwidth, with a frequency offset of 20 MHz. WLAN signals use OFDM modulation and have a nominal bandwidth of 20 MHz and 52 active sub-carriers. Various modulation types including BPSK, QPSK, 16 QAM and 64 QAM are used for each sub-carrier to provide flexibility for improving system capacity and ensuring system capability [23]. Two configurations of zero-IF and low-IF WLAN signals were used in the ACPR measurements: (i) 64 QAM OFDM modulation with 54 Mbps data rate and (ii) QPSK OFDM modulation with 36 Mbps data rate.

The upper and lower sideband ACPR are also symmetrical for the zero-IF OFDM case because the modulator has no significant memory. The lower sideband ACPR results for 64 QAM OFDM modulated zero-IF WLAN and QPSK OFDM modulated zero-IF WLAN against output power were plotted in Fig. 12. Note that the ACPR for the two zero-IF WLAN signals are close because they have similar PAR.

The measured and modelled upper and lower sideband ACPR results for 64 QAM OFDM modulated low-IF

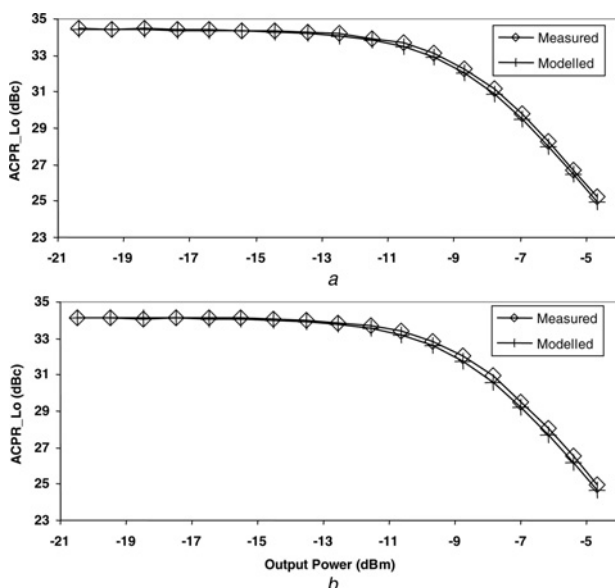


**Figure 12** Measured and modelled ACPR (lower sideband)

a Zero-IF WLAN signal with 64 QAM OFDM modulation  
b Zero-IF WLAN signal with QPSK OFDM modulation

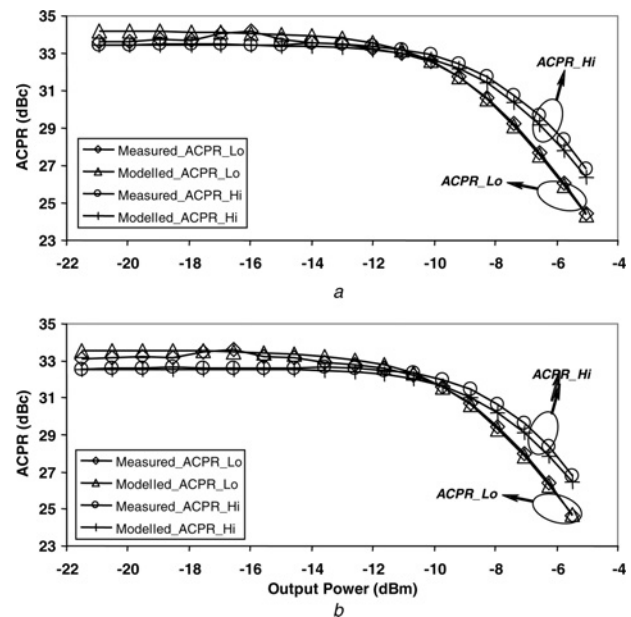


**Figure 13** Measured and modelled ACPR (ACPR<sub>Hi</sub> – ACPR upper sideband; ACPR<sub>Lo</sub> – ACPR lower sideband)

a Low-IF WLAN signal with 64 QAM OFDM modulation  
b Low-IF WLAN signal with QPSK OFDM modulation

WLAN and QPSK OFDM modulated low-IF WLAN against output power were shown in Fig. 13. Owing to the third order harmonics shift as explained in Section 2.3.1, the lower and upper sideband ACPR for the low-IF WLAN signals are asymmetrical. For both zero-IF and low-IF WLAN signals, the differences between the measured and modelled ACPR are close within 1 dB, which proves that the modulator non-linear behavioural model is accurate for estimating the out-of-band distortion in both applications.

## 5 Conclusion

In this paper, we extend our previous non-linear behavioural model of direct conversion quadrature modulators [9] which characterises only non-linear distortion to a more complete model for accurate characterisation of not only non-linear distortion, but also DC offset and gain/phase imbalance in modulators. In the new model, the non-linear coefficients were extracted by an offset sinusoidal AM–AM and AM–PM measurement and the linear error coefficients were extracted by a straightforward four-point VNA measurement. The linear model portion was validated by CL and IRR measurements, and the non-linear model portion was validated by ACPR measurements using WCDMA, zero-IF WLAN and low-IF WLAN signals. Moreover, in this work, the impact of physical impairments on quadrature modulators, including non-linear distortion, DC offset and gain/phase imbalance was investigated for three different application scenarios of quadrature modulators: DSB modulation, zero-IF SSB OFDM modulation and low-IF SSB OFDM modulation systems. The analysis results were validated by EVM measurements.

## 6 References

- [1] SANTOS R.E., CARVALHO N.B., GARD K.: 'Characterization of SNDR degradation in nonlinear wireless transmitters', *Int. J. RF Microw. Comput. Aided Eng.*, 2009, **19**, (4), pp. 470–480
- [2] DING L., MA Z., MORGAN D.R., ZIERDT M., ZHOU G.T.: 'Frequency-dependent modulator imbalance in predistortion linearization systems: modeling and compensation'. 2003 Asilomar Conf. on Signals, Systems and Computers, November 2003, pp. 688–692
- [3] ZHU Z., HUANG X.: 'Bias analysis of a gain/phase/dc-offset estimation technique for direct frequency conversion modulators'. IEEE Int. Conf. on Acoustics, Speech and Signal, March 2005, vol. 3, pp. 825–828
- [4] HEITER G.L.: 'Characterization of nonlinearities in microwave devices and systems', *IEEE Trans. Microw. Theory Tech.*, 1973, **21**, (12), pp. 797–805
- [5] PEDRO J.C., MA S.A.: 'A comparative overview of microwave and wireless power-amplifier behavioral modeling approaches', *IEEE Trans. Instrum. Meas.*, 2005, **53**, pp. 1150–1163
- [6] GARD K.G., LARSON L.E., STEER M.B.: 'The impact of RF front-end characteristics on the spectral regrowth of communication signals', *IEEE Trans. Microw. Theory Tech.*, 2005, **53**, (6), pp. 2179–2186
- [7] ARNO P., LAUNAY F., FOURNIER J.M., GRASSET J.C.: 'A simple method based on AM–AM, AM–PM measurements and CDMA signal statistics for RF power amplifier characterization'. 47th Midwest Symp. on Circuits and Systems, July 2004, vol. 3, pp. 1–4
- [8] GHARAIBEH K.M., STEER M.B.: 'Modeling distortion in multichannel communication systems', *IEEE Trans. Microwave Theory Tech.*, 2005, **53**, (5), pp. 1682–1692
- [9] LI M., HOOVER L., GARD K.G., STEER M.B.: 'Behavioral modeling for I/Q quadrature modulators for characterization of nonlinear distortions'. 2006 Int. Microwave Symp., June 2006, pp. 552–555
- [10] ZANNOTH M., RUHLICKE T., KLEPSE B.-U.: 'A highly integrated dual-band multimode wireless LAN transceiver', *IEEE J. Solid-State Circuits*, 2004, **39**, (7), pp. 1191–1195
- [11] HELAOUI M., BOUMAIZA S., GHAZEL A., GHANNOUCHI F.M.: 'On the RF/DSP design for efficiency of OFDM transmitters', *IEEE Trans. Microw. Theory Tech.*, 2005, **53**, (7), pp. 2355–2361
- [12] WINDISCH M., FETTWEIS G.: 'Adaptive I/Q imbalance compensation in low-IF transmitter architectures'. IEEE 60th Vehicular Technology Conf., 2004, vol. 3, pp. 2096–2100
- [13] GHARAIBEH K.M., GARD K.G., STEER M.B.: 'In-band distortion of multisines', *IEEE Trans. Microw. Theory Tech.*, 2006, **54**, pp. 3227–3236
- [14] PEDRO J.C., CARVALHO N.B.: 'On the use of multitone techniques for assessing RF components' intermodulation distortion', *IEEE Trans. Microw. Theory Tech.*, 1999, **47**, pp. 2393–2402
- [15] APARIN V.: 'Analysis of CDMA signal spectral regrowth and waveform quality', *IEEE Trans. Microw. Theory Tech.*, 2001, **49**, (12), pp. 2306–2314
- [16] OCHIAI H., IMAI H.: 'On the distribution of the peak-to-average power ratio in OFDM signals', *IEEE Trans. Commun.*, 2001, **49**, (2), pp. 282–289
- [17] Third Generation Partnership Project: 'Technical specification group radio access network; base station conformance testing (FDD) release 5'. 3GPP Technical Specification 25.141, V5.4.0 (2002–09)
- [18] CUTLER B.: 'Effects of physical layer impairments on OFDM systems', *RF Des. Mag.*, 2002, pp. 36–44
- [19] GHARAIBEH K.M., GARD K.G., STEER M.B.: 'Accurate estimation of digital communication system metrics – SNR, EVM and Rho in a nonlinear amplifier environment'. 64th ARFTG Microwave Measurements Conf., December 2004, pp. 41–44
- [20] MARSILI S.: 'DC offset estimation in OFDM based WLAN application'. 2004 IEEE Global Telecommunications Conf., December 2004, vol. 6, pp. 3531–3535
- [21] RAZAVI B.: 'RF microelectronics' (Prentice-Hall, New Jersey, 1998)
- [22] Third Generation Partnership Project: 'User Equipment (UE) radio transmission and reception (FDD)'. 3GPP Technical Specification 25.101, V5.11.0 (2004–06)
- [23] Institute of Electrical and Electronics Engineers, Inc., IEEE Std 802.11g-2003: 'Part 11: Wireless LAN Medium Access Control (MAC) and Physical Layer (PHY) specifications Amendment 4: further higher data rate extension in the 2.4 GHz band', 27 June 2003